Respiratory Self-navigated Postcontrast Whole-Heart Coronary MR Angiography: Initial Experience in Patients[1]

Davide Piccini, MSc
Pierre Monney, MD
Christophe Sierro, MD
Simone Coppo, MSc
Gabriele Bonanno, MSc
Ruud B. van Heeswijk, PhD
Jérôme Chaptinel, MSc
Gabriella Vincenti, MD
Jonathan de Blois, MD
Simon C. Koestner, MD
Tobias Rutz, MD
Arne Littmann, PhD
Michael O. Zenge, PhD
Juerg Schwitter, MD
Matthias Stuber, PhD

Purpose: To assess the diagnostic performance of respiratory self-navigation for whole-heart coronary magnetic resonance (MR) angiography in a patient cohort referred for diagnostic cardiac MR imaging.

Materials and Methods: Written informed consent was obtained from all participants for this institutional review board–approved study. Self-navigated coronary MR angiography was performed after administration of a contrast agent in 78 patients (mean age, 48.5 years ± 20.7 [standard deviation]; 53 male patients) referred for cardiac MR imaging because of coronary artery disease (n = 40), cardiomyopathy (n = 14), congenital anomaly (n = 17), or "other" (n = 7). Examination duration was recorded, and the image quality for each coronary segment was assessed with consensus reading. Vessel sharpness, length, and diameter were measured. Quantitative values in proximal, middle, and distal segments were compared by using analysis of variance and t tests. A double-blinded comparison with the results of x-ray angiography was performed when such results were available.

Results: When patients with different indications for cardiac MR imaging were examined with self-navigated postcontrast coronary MR angiography, whole-heart data sets with 1.15-mm isotropic spatial resolution were acquired in an average of 7.38 minutes ± 1.85. The main and proximal coronary segments could be visualized in 92.3% of cases, while the middle and distal segments could be visualized in 84.0% and 55.8% of cases, respectively. Subjective scores and vessel sharpness were significantly higher in the proximal segments than in the middle and distal segments ($P < .05$). Anomalies of the coronary arteries could be confirmed or excluded in all cases. Per-vessel sensitivity and specificity for stenosis detection were 64.7% and 85.0%, respectively, in the 31 patients for whom reference standard x-ray coronary angiography results were available.

Conclusion: The self-navigated coronary MR angiography sequence shows promise for coronary imaging. However, technical improvements are needed to improve image quality, especially in the more distal coronary segments.

Online supplemental material is available for this article.

[1] From Advanced Clinical Imaging Technology, Siemens Healthcare IM BM PI, Lausanne, Switzerland (D.P.); Department of Radiology, University Hospital and University of Lausanne, Lausanne, Switzerland (D.P., S.C., G.B., R.B.v.H., J.C., M.S.); Center for Biomedical Imaging, Centre Hospitalier Universitaire Vaudois, rue de Bugnon 46, BH 8.80, 1011 Lausanne, Switzerland (D.P., S.C., G.B., R.B.v.H., J.C., M.S.); Pattern Recognition Laboratory, Department of Computer Science, Friedrich-Alexander University of Erlangen-Nuremberg, Erlangen, Germany (D.P.); Division of Cardiology and Cardiac MR Center, University Hospital of Lausanne, Lausanne, Switzerland (P.M., C.S., G.V., J.d.B., S.C.K., T.R., J.S.); and MR Research and Development (A.L.), MR Product Innovation and Definition (M.O.Z.), Healthcare Sector, Siemens, Erlangen, Germany. Received August 29, 2013; revision requested September 16; revision received September 30; accepted October 4; final version accepted October 9. **Address correspondence to** M.S. (e-mail: *Matthias.Stuber@chuv.ch*).

Whole-heart coronary magnetic resonance (MR) angiography has become an appealing alternative to x-ray or computed tomographic (CT) coronary angiography, as it is noninvasive and safe, can be easily repeated, and operates without ionizing radiation (1). Considering that a substantial minority of patients who undergo invasive x-ray coronary angiography are found to have no clinically important luminal coronary artery disease (CAD) (2,3), coronary MR angiography may play an important role in patient care.

Coronary MR angiography is usually electrocardiographically triggered to avoid image artifacts caused by the periodic contraction and relaxation of the heart. Image data are typically acquired over a large number of heartbeats and during a short time window in the cardiac cycle. To account for respiratory motion, a navigator (4) is commonly placed at the dome of the right hemidiaphragm and is used for both gating and real-time tracking of the imaged volume position. Although major improvements have been reported in recent years (5–8), and selected single-center studies have demonstrated that the sensitivity and specificity of this technique approach that of CT (9–11), a number of rate-limiting steps still exist and preclude more widespread use of this technique. First, user-dependent navigator placement and irregular patient breathing patterns lead to variable and unpredictable imaging times (1) and sometimes even failure to complete an examination (7). Second, respiratory displacement measured at the level of the diaphragm is only indirectly linked with that of the heart, this relationship may change during an examination, and both hysteretic effects (12) and temporal delays (13) have been reported as additional complications. In response, respiratory self-navigation has recently been introduced (14) for coronary MR angiography. With this technique, respiratory motion data are directly extracted at the level of the heart and from the k-space data acquired for coronary imaging. This avoids an indirect measurement and makes the technique theoretically less vulnerable to changes in breathing patterns, while adverse effects related to hysteresis or temporal delays can be avoided. Simultaneously, navigator placement is no longer needed, imaging time depends only on the heart rate of the patient, and, by using a three-dimensional (3D) radial approach, isotropic spatial resolution is achieved without "foldover" artifacts. While the first in vivo human results in small cohorts of healthy adult volunteers have been reported earlier (14–17), the diagnostic performance of this approach in patients suspected of having CAD has not been ascertained previously, to our knowledge. Therefore, the purpose of this study was to assess the diagnostic performance of respiratory self-navigation for whole-heart coronary MR angiography in a patient cohort referred for diagnostic cardiac MR imaging.

Advances in Knowledge

- Respiratory self-navigation can be successfully applied for whole-heart coronary MR imaging in a nonselected patient cohort.
- Image quality is satisfactory for the routine visualization of the main and proximal coronary segments, although technical improvements are needed to improve image quality in the distal segments.
- The quality of the coronary images is sufficient to enable discrimination between normal and anomalous coronary arteries; however, the sensitivity (64.7%) for detecting proximal coronary artery stenoses still needs to be improved.

Implications for Patient Care

- The self-navigated three-dimensional radial pulse sequence significantly improves the ease of use of coronary MR imaging in a patient setting, because no navigators are needed and "foldover" is not a concern.
- Because the acquisition time is known a priori and does not depend on the breathing pattern, this sequence can be introduced within a routine clinical cardiac protocol.

Materials and Methods

One of the authors (D.P.) is an employee of Siemens Healthcare (Lausanne, Switzerland), while two authors (A.L. and M.O.Z.) are employees of Siemens Healthcare (Erlangen, Germany). Authors who were not employees of or consultants for Siemens had control of inclusion of any data and information that might present a conflict of interest for the authors who are industry employees.

Study Population

A total of 78 patients with a mean age of 48.5 years ± 20.7 (standard deviation) and an age range of 8–82 years (53 male patients [mean age, 50.0 years ± 19.3; range, 14–82 years] and 25 female patients [mean age, 45.4 years ± 23.4; range, 8–79 years]) were examined. There was no significant difference in age between the male and the female patients (P = .371, two-sample

Published online before print
10.1148/radiol.13132045 **Content codes:** CA MR

Radiology 2014; 270:378–386

Abbreviations:
CAD = coronary artery disease
CI = confidence interval
LAD = left anterior descending
LCX = left circumflex
OR = odds ratio
RCA = right coronary artery
3D = three-dimensional

Author contributions:
Guarantors of integrity of entire study, D.P., J.S., M.S.; study concepts/study design or data acquisition or data analysis/interpretation, all authors; manuscript drafting or manuscript revision for important intellectual content, all authors; manuscript final version approval, all authors; literature research, D.P., C.S., J.S., M.S.; clinical studies, D.P., P.M., C.S., G.V., S.C.K., T.R.; experimental studies, D.P., S.C., G.B., R.B.v.H., J.C., J.d.B., T.R., M.O.Z.; statistical analysis, D.P., S.C., G.B., R.B.v.H., J.C., A.L., M.S.; and manuscript editing, D.P., S.C., G.B., R.B.v.H., J.d.B., S.C.K., T.R., A.L., M.O.Z., M.S.

Conflicts of interest are listed at the end of this article.

two-tailed Student *t* test). The average body mass index was 24.3 kg/m^2 ± 4.6. Patients were referred for cardiac MR imaging because they were known to have or were suspected of having CAD (n = 40), for evaluation of congenital coronary anomalies (n = 17), for evaluation of cardiomyopathy (n = 14), and for other reasons (n = 7). All patient indications are reported in Table 1. In the current study, no specific exclusion criteria were applied, and the MR angiography data sets in all 78 patients were included in the final quantitative analyses. This study was approved by the local ethics committee at the University Hospital in Lausanne (Commission cantonale d'éthique de la recherche sur l'être humain).

Table 1

Indications for Cardiac MR Imaging for 78 Patients

Indication	Stress Perfusion	MR Angiography	Late Gadolinium Enhancement	X-Ray Angiography
Suspected CAD (n = 18)	18/18	2/18	18/18	2/18
Confirmed CAD–ischemia (n = 11)	11/11	0/11	11/11	9/11
Confirmed CAD–viability (n = 11)	0/11	0/11	11/11	10/11
Cardiomyopathy (n = 14)	0/14	1/14	14/14	5/14
Congenital anomaly (n = 16)	1/16	15/16	7/16	1/16
Coronary abnormality (n = 1)	0/1	0/1	1/1	1/1
Other (n = 7)	0/7	3/7	5/7	3/7
Total (n = 78)	30/78	21/78	67/78	31/78

Note.—The patient cohort was subdivided into seven categories of common indications for cardiac MR imaging. The examinations were the specific examinations performed for diagnosis in the specific patients, although they were not the only examinations undergone by the patients. In all patients, standard localizers were obtained and two-dimensional cine imaging for ejection fraction calculation was performed. "Other" = for example, work-up of valvular disease or right ventricular assessment in pulmonary hypertension.

Coronary MR Angiography Data Acquisition

All examinations were performed with a 1.5-T clinical MR imaging unit (MAGNETOM Aera; Siemens, Erlangen, Germany). Thirty elements of the anterior and posterior phased-array coils were activated for signal reception. Data acquisition was performed by using a 3D radial trajectory with a spiral phyllotaxis pattern (18) (Fig E1a [online]), adapted for self-navigation as described in (15) (Fig E1b and E1c [online]). The self-navigated study did not require any extra localizer, and the planning of the whole-heart acquisition included only the placement of the cubic field of view around the heart as seen on the very first scout image used for cardiac imaging. A saturation slab at the level of the anterior chest wall was also localized on this scout image. Motion detection and correction and image reconstruction were performed automatically and in real time on the console of the system. All measurements were performed by using k-space segmentation and electrocardiographic triggering. For the acquisition of each k-space segment, both T2 preparation (echo time, 40 msec) (19) and fat saturation were added prior to balanced steady-state free precession image data acquisition. In all patients, a total dose of 0.2 mmol gadobutrol (Gadovist; Bayer Schering Pharma, Zurich, Switzerland) per kilogram of body weight was administered. Specifically, the dose was injected as a single bolus of 0.2 mmol/kg for viability assessment (n = 27) or for angiography of the great vessels (n = 11); as a single bolus of 0.1 mmol/kg each for viability assessment and angiography (n = 10); or as a bolus of 0.1 mmol/kg for first-pass myocardial perfusion assessment during adenosine stress, followed by a bolus of 0.1 mmol/kg at rest (n = 30). Immediately after administration of the total dose, stacks of axial, sagittal, and coronal volume interpolated breath-hold examination images were acquired for assessment of the thoracic anatomy. After the acquisition of these anatomic images (ie, approximately 4 minutes after the last injection), the 3D self-navigated imaging was performed with the following parameters: repetition time msec/echo time msec, 3.1/1.56; field of view, 220 × 220 × 200 mm; matrix, 192 × 192 × 192; acquired voxel size, 1.15 × 1.15 × 1.15 mm; radiofrequency excitation angle, 115°; and receiver bandwidth, 900 Hz/pixel. A total of approximately 15 000 radial readouts were acquired in 377 heartbeats (acquisition window, 100 msec) or in 610 heartbeats (acquisition window, 75 msec), depending on the individual heart rate of each patient (20), and with an overall sampling ratio of 20% of the Nyquist limit. The trigger delay was set by the cardiologist operating the MR imaging unit (J.S., with 18 years of experience in cardiac MR imaging; P.M., with 4 years of experience; G.V., with 5 years of experience; or T.R., with 3 years of experience) by using visual inspection of the most quiescent middiastolic period on a midventricular short-axis cine image series acquired before the injection of the contrast agent. The heart rate of all patients was recorded during the routine two-dimensional cine acquisitions before contrast agent injection and was used to compute the expected duration of the self-navigated whole-heart acquisition. The actual duration of the whole-heart acquisition was assessed for comparison.

Coronary Arteries and Image Quality

The proximal, middle, and distal segments of the right coronary artery (RCA), the left anterior descending (LAD) artery, and the left main stem and the proximal segment of the left circumflex (LCX) artery were identified and classified following the guidelines of the American Heart Association (21). All segments were graded on a five-point scale for image quality by two experts (M.S., with 17 years of experience in coronary MR angiography, and D.P., with 5 years of experience). The five-point scale was adapted from that used by McConnell et al (22) by using consensus reading, as proposed by Kim and colleagues (23). The scale

grades border definition of the coronary arteries as follows: A score of 0 indicates not visible; a score of 1, markedly blurred; a score of 2, moderately blurred; a score of 3, mildly blurred; and a score of 4, sharply defined. Any segment with a grade higher than 0 was considered to be visualized. The two experts were blinded completely to patient indications and clinical conditions. The percentage vessel sharpness was then also computed for all the visualized coronary segments (by S.C., G.B., and R.B.v.H., all with 3 years of experience in coronary MR angiography) by using an approach similar to that described by Etienne et al (24). Visual vessel length was measured (by D.P., with 5 years of experience in coronary MR angiography) for both the right and the left coronary systems by using CoronaViz (a work-in-progress software by Siemens Corporate Research, Princeton, NJ). Vessel diameter was computed for all visualized coronary segments.

Diagnostic Performance for Detection of CAD

On the MR images, a double-blinded evaluation for the detection of significant luminal coronary disease in the left main stem, the RCA, the LAD artery, and the proximal LCX artery was performed for all patients by consensus reading. The observers (M.S. and D.P.) did not know whether an x-ray coronary angiogram would be available for comparison in a given patient, nor did they know the specific indication for cardiac MR imaging. The stenoses on x-ray angiograms were independently identified and graded (a stenosis > 50% of the vessel diameter was considered to be significant) by an experienced cardiologist (C.S., with 10 years of experience in x-ray coronary angiography). After unblinding, sensitivity and specificity were computed for the proximal and middle segments of the coronary vessels that were available for analysis with both modalities. Results of per-patient, per-vessel, and per-segment analyses are reported.

Statistical Analysis

To assess any significant difference in image quality between coronary segments, all segments were sorted into one of three groups: proximal (including the left main stem and the proximal RCA, LCX artery, and LAD artery), middle (including the middle RCA and LAD artery), and distal (including the distal RCA and LAD artery).

Quality grades and percentages of vessel sharpness were compared among the three groups as follows: First, a one-way analysis of variance was used to test whether an effect was present among the means of the three groups. $P < .05$ was considered to indicate a statistically significant difference. When an effect was found, multiple paired two-tailed Student t tests were performed, with a $P < .017$ considered to indicate a significant difference after Bonferroni adjustment for multiple comparisons (.05/3), as described by Tello and Crewson (25).

As for vessel visualization (grade > 0), the odds of being visualized or nonvisualized were computed for each group. Odds ratios (ORs) and their 95% confidence intervals (CIs) were then computed among the three groups, as described previously (26). All statistical analyses were performed with Excel 2007 (Microsoft, Bothell, Wash), except for the analysis of variance tests, which were performed in Matlab v7.13 (Mathworks, Natick, Mass). Sensitivity and specificity values were calculated by using Excel 2007.

Results

In the patient population studied, the prevalence of cardiovascular risk factors was in line with that of a population known to have or suspected of having CAD, with 30.8% (n = 24) of patients having systemic arterial hypertension (50.0% [n = 39] of patients did not have it, and in 19.2% [n = 15], hypertensive status was unknown), 25.7% (n = 20) of patients having hypercholesterolemia (53.8% [n = 42] of patients did not have it, and in 20.5% [n = 16], hypercholesterolemic status was unknown). There was a somewhat lower prevalence of other risk factors (eg, 10.3% [n = 8] of patients had diabetes mellitus, 14.1% [n = 11] had a positive family history of CAD, and 15.4% [n = 12] were smokers). In all patients, coronary MR angiography data acquisition was successfully completed. The average predicted acquisition time, based on the heart rate measured during the cine acquisitions, was 7.38 minutes ± 1.85, and the measured time for the 3D whole-heart self-navigated protocol was 7.84 minutes ± 1.88. A high linear correlation and an almost unitary slope (R^2 = 0.88, slope = 0.95) were found between the expected and the measured imaging times for all patients, as shown on the scatterplot in Figure E2 (online).

Coronary Arteries and Image Quality

The number of visualized coronary segments, the average quality grades, vessel sharpness, vessel length, and vessel diameter for all coronary segments are reported in Table 2. The quality grades and the vessel sharpness of the left main stem, the proximal LAD artery, and the proximal and middle RCA were, on average, higher than those of the respective distal segments. The image quality in the proximal and middle segments allowed assessment or exclusion of the anomalous origin and course of the coronary arteries, with respect to the anatomy of the heart and the great vessels, in all of the cases of coronary anomaly. Examples are displayed in Figure 1 and in Figure E3 (online). Finally, one of the patients had a saphenous vein graft to the distal LCX artery that was well reformatted and visualized in the 3D self-navigated data set and could be directly compared with the findings on the corresponding x-ray angiogram, as shown in Figure E4 (online).

Diagnostic Performance for Detection of CAD

After unblinding, it was found that x-ray coronary angiograms were available for 31 of the 78 patients. Two data sets were excluded from the analysis because of the low image quality of the MR angiograms (quality grade = 0), on which the coronary arteries could not be visualized. For the remaining 29 patients, the majority of the x-ray angiograms were obtained before (n = 22)

Table 2

Quantitative Results for Image Quality of the Coronary Arteries in 78 Patients

Parameter	Left Main Stem*	Proximal LCX Artery†	LAD Artery‡			RCA§		
			Proximal	Middle	Distal	Proximal	Middle	Distal
No. of patients in whom segments could be visualized	76/78	65/78	71/78	61/78	44/78	76/78	70/78	43/78
Grade	2.0 ± 0.9	1.2 ± 0.8	1.8 ± 1.1	1.3 ± 0.9	0.7 ± 0.7	1.8 ± 1.0	1.5 ± 1.0	0.7 ± 0.5
Sharpness (%)	42.0 ± 11.6	39.2 ± 8.9	39.5 ± 10.2	35.2 ± 10.3	37.2 ± 10.0	37.5 ± 12.8	36.6 ± 11.8	24.2 ± 7.5
Diameter (mm)	3.5 ± 0.6	3.1 ± 0.5	2.9 ± 0.5	3.0 ± 0.5	2.9 ± 0.6	3.0 ± 0.8	2.8 ± 0.6	2.9 ± 0.7

Note.—Data are means ± standard deviations.

* Average total sampled length = 16.6 mm ± 4.5.

† Average total sampled length = 31.0 mm ± 21.9.

‡ Average total sampled length = 68.6 mm ± 33.4.

§ Average total sampled length = 82.0 mm ± 41.1.

Figure 1

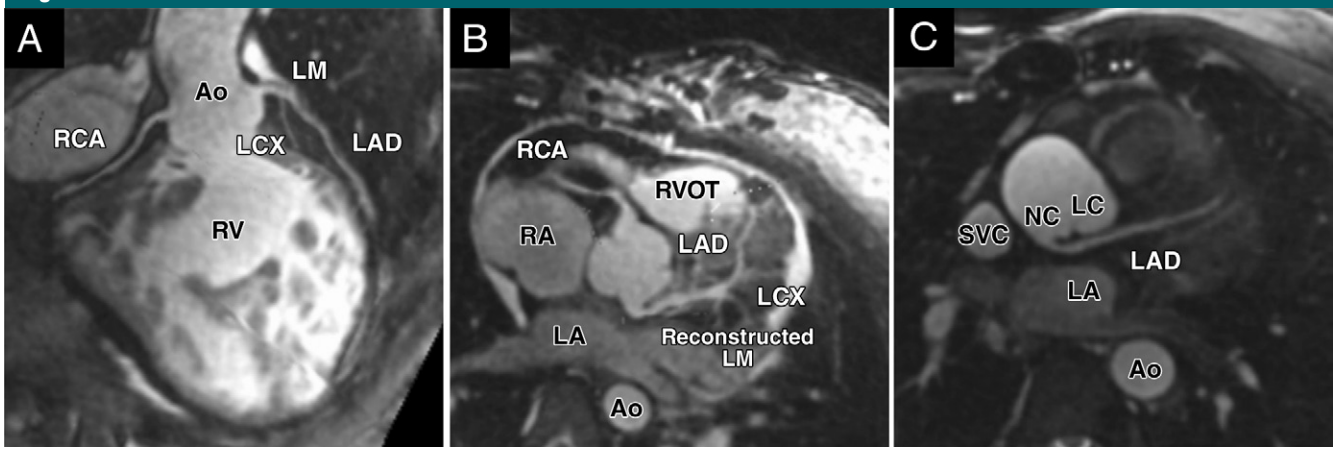

Figure 1: *A–C,* Examples of multiplanar reformats in the coronary arteries obtained offline from the whole-heart self-navigated MR angiography data sets. These reformats robustly depict the coronary arteries in relation to the neighboring anatomy. *A,* Normal coronary arteries in a case of transposition of the great arteries. The aorta is connected to the morphologic right ventricle. *B,* Reformat in a surgically reconstructed left main stem in a case of a syndrome of abnormal left coronary artery arising from the pulmonary artery. *C,* Abnormal left coronary artery arising from the noncoronary sinus and running between the aorta and the left atrium. *Ao* = aorta, *LA* = left atrium, *LC* = left coronary cusp, *LM* = left main stem, *NC* = noncoronary cusp, *RA* = right atrium, *RV* = right ventricle, *RVOT* = right ventricular outflow tract, *SVC* = superior vena cava.

the MR angiography examination (n = 2 on the same day, n = 5 MR angiography first). Among these patients, three had a time gap of more than 90 days with respect to the MR angiography examination, while the average time between the two examinations was 45 days. The left main stem and the RCA were assessed on all 29 x-ray angiograms, while angiograms of the LAD and LCX arteries were available for 28 patients. The double-blinded comparison of self-navigated whole-heart coronary MR angiography with x-ray angiography resulted in an overall per-patient sensitivity and specificity of 71.4% (15 of 21) and 62.5% (five of eight), respectively, for the detection of significant CAD in the proximal and middle segments. The total per-vessel sensitivity and specificity in the proximal and middle segments of the coronary vessels were 64.7% (22 of 34) and 85.0% (68 of 80), respectively, for the total of 114 coronary vessels examined. The values for each vessel are reported separately in Table 3. Considering the proximal and middle segments of each coronary artery separately, sensitivity and specificity reached an overall per-segment value of 46.2% and 82.6%, respectively. In Figure 2, example reformats of the left and right coronary systems obtained with the 3D self-navigated approach (Fig 2, *A, C, E*) in patients with CAD at x-ray angiography are displayed. The corresponding x-ray coronary angiograms are shown in Figure 2, *B, D, F.*

Table 3

Sensitivity and Specificity of Proposed Technique for Detection of CAD as Compared with X-Ray Angiography

Comparison Basis	Sensitivity (%)	Specificity (%)
Per patient	71.4 (15/21)	62.5 (5/8)
Per vessel (total)	64.7 (22/34)	85.0 (68/80)
Left main stem	50.0 (1/2)	96.3 (26/27)
LAD artery (proximal plus middle segments)	66.7 (10/15)	92.3 (12/13)
LCX (proximal plus middle segments)	33.3 (1/3)	88.0 (22/25)
RCA (proximal plus middle segments)	71.4 (10/14)	53.3 (8/15)
Per segment	46.2 (18/39)	82.6 (109/132)

Note.—Data in parentheses are raw data.

Statistical Analysis

The mean grades for the proximal, middle, and distal segment groups were 1.7 ± 1.0, 1.4 ± 1.0, and 0.7 ± 0.8, respectively. The average percentage vessel sharpness values for the proximal, middle, and distal segment groups were 39.5 ± 11.2, 35.9 ± 11.1, and 29.1 ± 10.6, respectively. In both cases, the analysis of variance test revealed a significant effect ($P < .0001$). At t testing, a statistical difference was found among all three groups for both quality grades and vessel sharpness ($P < .017$).

A proximal coronary segment was found to be 2.3 times more likely to be visualized when compared with the middle segments (OR = 2.3; 95% CI: 1.3, 4.2). A middle coronary segment was 4.2 times more likely to be visualized with respect to a distal segment (OR = 4.2; 95% CI: 2.4, 7.1), while the visualization ratio between proximal and distal segments was 9.5 (OR = 9.5; 95% CI: 5.6, 16.1). All of these values were found to be statistically significant, according to the observations of Medina and Zurakowski (26).

Discussion

In the present study, the respiratory self-navigated sequence resulted in a per-vessel specificity that was comparable to the values reported in the literature for conventional navigator-gated coronary MR angiography (85%), while the sensitivity (64.7%) was still lower. Main and proximal coronary segments could be visualized significantly more often than middle and distal segments (in 92.3% vs 84.0% and 55.8% of patients, respectively). The subjective scores and vessel sharpness were also significantly higher ($P < .05$) in the main and proximal segments with respect to their distal counterparts, and anomalies of the coronary arteries could be confirmed or excluded in all cases. Data acquisition was successful in all patients, while the total imaging time showed a high correlation with that predicted using the heart rate of the patients. While changes in the respiratory pattern or diaphragmatic drift have been a reason for termination of the examination or inability to reconstruct an image in navigator-gated acquisitions in the past (7), this no longer applies for self-navigated coronary MR angiography. Because the only determinant of acquisition duration is the heart rate of the patient, the imaging duration is known a priori, which is most useful for protocol definition. Data accepted for reconstruction originate from a large range of respiratory displacements, and thus, a change in the orientation or shape of the heart between respiratory phases is more likely. However, the current reconstruction algorithm does not account for these effects. For these reasons, an image reconstruction technique that excludes image data acquired during outlier respiratory positions, may lead to an improvement in image quality.

While discussing the average grades for each coronary segment obtained in this study, some important aspects should be considered. First, the grading performed by the two experts was completely blinded with respect to the specific patient indication for imaging and medical condition. In other words, low grades for specific coronary segments were given regardless of the underlying reason for the suboptimal visualization (eg, suboptimal performance of the self-navigated sequence, presence of a stent, presence of disease or calcifications). Second, the patient group was varied and representative of an unselected cohort of patients that may routinely be referred for cardiac MR imaging. All age, weight, and size categories were included, no exclusion criteria (eg, extrasystole, irregular breathing) were applied, and the acquisition was planned by several different operators with training in general cardiac MR imaging but no special training on the use of the self-navigated sequence. Although image quality was, on average, satisfactory for the visualization of the proximal segments of the coronary tree, the method still needs to be improved for better visualization of more distal parts. Residual, unsuppressed cardiac motion and residual 3D respiratory displacement are likely causes of image quality degradation. In particular, we have exploited respiratory motion correction in only the superior-inferior direction. However, it is has been documented (27) that this motion is more complex and individually dependent. Therefore, future developments should be directed toward 3D motion correction. Because the 3D radial k-space sampling scheme enables respiratory motion correction in any direction, an expansion to 3D motion correction seems straightforward and holds promise for further improvements in image quality (17). Moving forward, a combination of compressed sensing (28) and either navigator gating or self-navigation may have advantages in terms of image quality and acquisition time.

Streaking artifacts due to radial undersampling are mainly caused by bright,

Figure 2

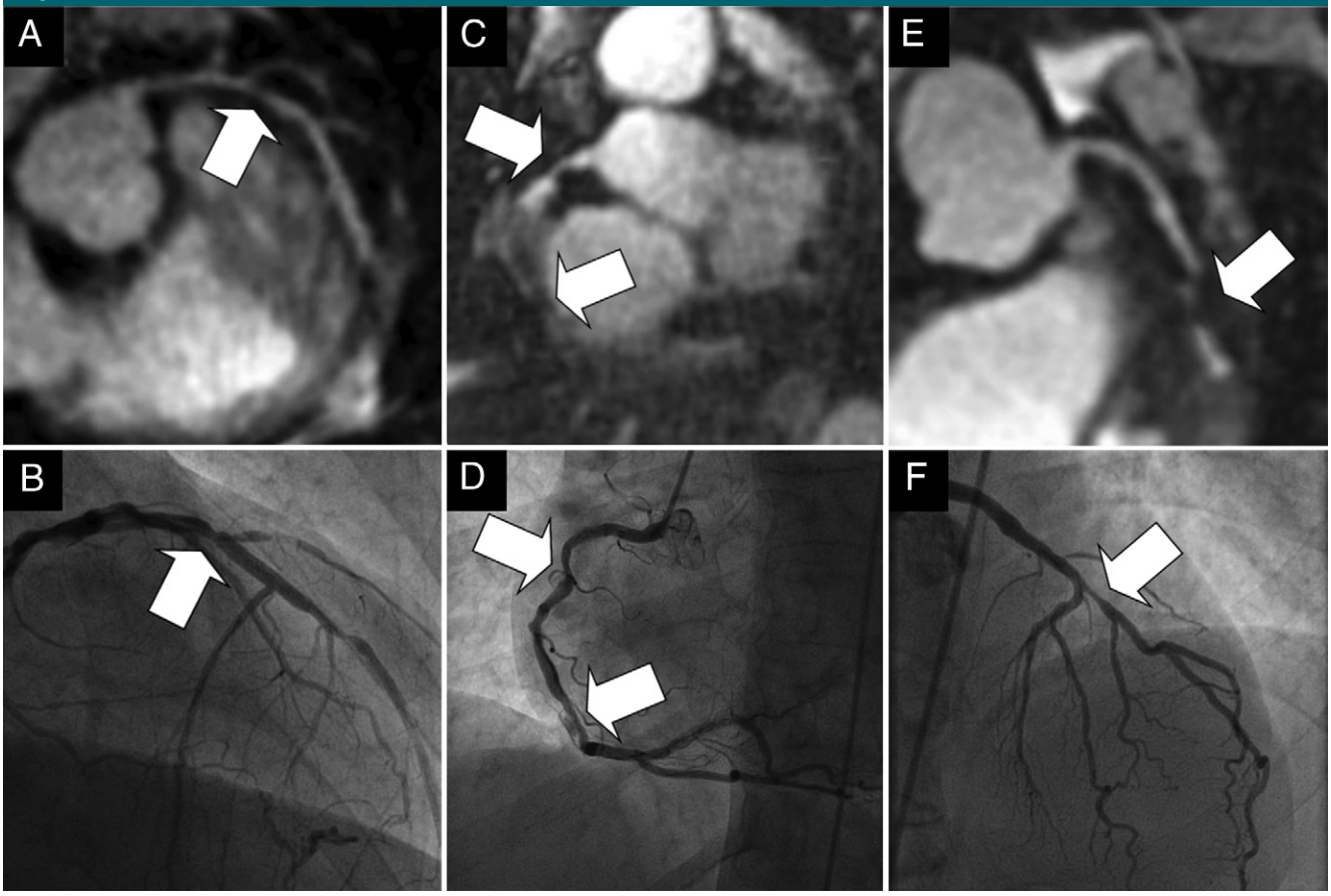

Figure 2: *A–F,* Examples of the comparison between multiplanar reformats of the whole-heart self-navigated coronary MR angiography data sets (top row) and the corresponding x-ray coronary angiograms (bottom row) in three patients. The lesion in the proximal LAD artery and just distal to the take-off of a diagonal branch can clearly be identified in the first patient in, *A,* while this is confirmed on the x-ray angiogram in, *B.* While the luminal narrowing of the proximal RCA in the second patient on, *C,* can clearly be identified, the further course of this artery is obscured in the region of a stent. The same interstent restenoses can be identified in, *D.* In the third patient in, *E,* significant disease is identified in the proximal LAD artery at MR angiography and is confirmed on, *F,* the corresponding x-ray coronary angiogram. Arrows = stenoses.

unsuppressed fat signal outside the field of view. An improved fat saturation strategy for radial sampling is therefore desirable. However, for radial approaches, fat saturation is more challenging, as each signal readout goes through the origin of k-space. Alternatively, the utility of spectral spatial pulses (29) remains to be investigated, but a prolonged repetition time may be expected. Finally, our study was performed at 1.5 T and without the administration of isosorbide dinitrate (30) or β-blockers.

The diagnostic accuracy of coronary MR angiography for the detection of CAD has been investigated in several single-center studies in recent years (8,23,31–35), resulting in sensitivities ranging from 73% to 97% and specificities ranging from 68% to 96%. In particular, the most recent multicenter trial (1) reported a per-vessel sensitivity and specificity of 83% and 90%, respectively. The current assessment of the performance of the self-navigated coronary MR angiography acquisition demonstrated a per-vessel specificity close to previously reported values, while the sensitivity was still suboptimal. However, in the majority of the above-mentioned studies, only patients who were scheduled to undergo or who had undergone x-ray coronary angiography for diagnostic purposes were selected for MR imaging. This leads to a certain selection bias that was not present in our study, because all 78 patients that were referred to cardiac MR imaging underwent a double-blinded analysis of the MR angiography data sets for detection of CAD. However, a certain bias was intrinsically unavoidable in the subset of patients whose data were used for the computation of sensitivity and specificity (because x-ray angiography was performed only in the setting of suspected or confirmed CAD). Nevertheless, only after unblinding did we learn about the specific cardiac MR imaging indications of each of the patients and which of them did

or did not have x-ray coronary angiographic data available for comparison.

While both imaging time and spatial resolution are still inferior for coronary MR angiography with respect to CT angiography (10,11), the ease of use of the former has also been limited because of the need for meticulous scout imaging, navigator placement, and uncertain imaging times. Respiratory self-navigation removes these barriers. Simultaneously, and as demonstrated, it can easily be integrated into a comprehensive cardiac examination that provides complementary information that may not as easily be obtained with contemporary CT angiography.

Our study had limitations. Because patients were not selected a priori for assessment of CAD in comparison with x-ray angiography, only a limited number of data sets with respect to the total (31 of 78) could be used for calculation of sensitivity and specificity for detecting coronary artery stenoses. The evaluation of the self-navigated coronary MR angiography technique in a preselected patient cohort has to be considered for future studies. Although image quality measures (eg, vessel sharpness) were reported, the self-navigated sequence was not directly compared with standard navigator-gated coronary MR angiography techniques. However, this has been reported in a small volunteer study previously (15). Nevertheless, a direct comparison between these techniques in patients with CAD will be of high interest.

The results of this study demonstrate that respiratory self-navigated whole-heart coronary MR angiography is feasible in a patient setting and can easily be performed after contrast agent administration. Specificity for CAD detection in proximal branches is promising, while sensitivity needs to be improved.

Acknowledgments: The authors thank all the members of the Center of Cardiac Magnetic Resonance team at the University Hospital of Lausanne and all the MR technologists for their valuable participation, helpfulness, and support during this study.

Disclosures of Conflicts of Interest: D.P. Financial activities related to the present article: none to disclose. Financial activities not related to the present article: is an employee of and holds patents with Siemens Healthcare. Other relationships: none to disclose. **P.M.** No relevant conflicts of interest to disclose. **C.S.** No relevant conflicts of interest to disclose. **S.C.** No relevant conflicts of interest to disclose. **G.B.** No relevant conflicts of interest to disclose. **R.B.v.H.** No relevant conflicts of interest to disclose. **J.C.** No relevant conflicts of interest to disclose. **G.V.** No relevant conflicts of interest to disclose. **J.d.B.** No relevant conflicts of interest to disclose. **S.C.K.** No relevant conflicts of interest to disclose. **T.R.** No relevant conflicts of interest to disclose. **A.L.** Financial activities related to the present article: none to disclose. Financial activities not related to the present article: is an employee of Siemens. Other relationships: none to disclose. **M.O.Z.** Financial activities related to the present article: none to disclose. Financial activities not related to the present article: is an employee of and owns stock in Siemens. Other relationships: none to disclose. **J.S.** Financial activities related to the present article: institution received a grant from Bracco and consulting fees or honoraria from Bayer Healthcare and Medtronic. Financial activities not related to the present article: none to disclose. Other relationships: none to disclose. **M.S.** Financial activities related to the present article: none to disclose. Financial activities not related to the present article: was a consultant to Diagnosoft until April 2011. Other relationships: none to disclose.

References

1. Kato S, Kitagawa K, Ishida N, et al. Assessment of coronary artery disease using magnetic resonance coronary angiography: a national multicenter trial. J Am Coll Cardiol 2010;56(12):983–991.
2. Dissmann W, de Ridder M. The soft science of German cardiology. Lancet 2002;359(9322):2027–2029.
3. Patel MR, Peterson ED, Dai D, et al. Low diagnostic yield of elective coronary angiography. N Engl J Med 2010;362(10):886–895.
4. Ehman RL, Felmlee JP. Adaptive technique for high-definition MR imaging of moving structures. Radiology 1989;173(1):255–263.
5. Weber OM, Martin AJ, Higgins CB. Whole-heart steady-state free precession coronary artery magnetic resonance angiography. Magn Reson Med 2003;50(6):1223–1228.
6. Bi X, Carr JC, Li D. Whole-heart coronary magnetic resonance angiography at 3 Tesla in 5 minutes with slow infusion of Gd-BOPTA, a high-relaxivity clinical contrast agent. Magn Reson Med 2007;58(1):1–7.
7. Sakuma H, Ichikawa Y, Suzawa N, et al. Assessment of coronary arteries with total study time of less than 30 minutes by using whole-heart coronary MR angiography. Radiology 2005;237(1):316–321.
8. Sakuma H, Ichikawa Y, Chino S, Hirano T, Makino K, Takeda K. Detection of coronary artery stenosis with whole-heart coronary magnetic resonance angiography. J Am Coll Cardiol 2006;48(10):1946–1950.
9. Sakuma H. Coronary CT versus MR angiography: the role of MR angiography. Radiology 2011;258(2):340–349.
10. Hamdan A, Asbach P, Wellnhofer E, et al. A prospective study for comparison of MR and CT imaging for detection of coronary artery stenosis. JACC Cardiovasc Imaging 2011;4(1):50–61.
11. Scheffel H, Stolzmann P, Alkadhi H, et al. Low-dose CT and cardiac MR for the diagnosis of coronary artery disease: accuracy of single and combined approaches. Int J Cardiovasc Imaging 2010;26(5):579–590.
12. Nehrke K, Börnert P, Manke D, Böck JC. Free-breathing cardiac MR imaging: study of implications of respiratory motion—initial results. Radiology 2001;220(3):810–815.
13. Spuentrup E, Manning WJ, Botnar RM, Kissinger KV, Stuber M. Impact of navigator timing on free-breathing submillimeter 3D coronary magnetic resonance angiography. Magn Reson Med 2002;47(1):196–201.
14. Stehning C, Börnert P, Nehrke K, Eggers H, Stuber M. Free-breathing whole-heart coronary MRA with 3D radial SSFP and self-navigated image reconstruction. Magn Reson Med 2005;54(2):476–480.
15. Piccini D, Littmann A, Nielles-Vallespin S, Zenge MO. Respiratory self-navigation for whole-heart bright-blood coronary MRI: methods for robust isolation and automatic segmentation of the blood pool. Magn Reson Med 2012;68(2):571–579.
16. Henningsson M, Koken P, Stehning C, Razavi R, Prieto C, Botnar RM. Whole-heart coronary MR angiography with 2D self-navigated image reconstruction. Magn Reson Med 2012;67(2):437–445.
17. Lai P, Bi X, Jerecic R, Li D. A respiratory self-gating technique with 3D-translation compensation for free-breathing whole-heart coronary MRA. Magn Reson Med 2009;62(3):731–738.
18. Piccini D, Littmann A, Nielles-Vallespin S, Zenge MO. Spiral phyllotaxis: the natural way to construct a 3D radial trajectory in MRI. Magn Reson Med 2011;66(4):1049–1056.
19. Brittain JH, Hu BS, Wright GA, Meyer CH, Macovski A, Nishimura DG. Coronary angiography with magnetization-prepared T2 contrast. Magn Reson Med 1995;33(5):689–696.
20. Plein S, Jones TR, Ridgway JP, Sivananthan MU. Three-dimensional coronary MR an-

giography performed with subject-specific cardiac acquisition windows and motion-adapted respiratory gating. AJR Am J Roentgenol 2003;180(2):505–512.

21. Austen WG, Edwards JE, Frye RL, et al. A reporting system on patients evaluated for coronary artery disease. Report of the Ad Hoc Committee for Grading of Coronary Artery Disease, Council on Cardiovascular Surgery, American Heart Association. Circulation 1975;51(4 Suppl):5–40.
22. McConnell MV, Khasgiwala VC, Savord BJ, et al. Comparison of respiratory suppression methods and navigator locations for MR coronary angiography. AJR Am J Roentgenol 1997;168(5):1369–1375.
23. Kim WY, Danias PG, Stuber M, et al. Coronary magnetic resonance angiography for the detection of coronary stenoses. N Engl J Med 2001;345(26):1863–1869.
24. Etienne A, Botnar RM, Van Muiswinkel AM, Boesiger P, Manning WJ, Stuber M. "Soap-bubble" visualization and quantitative analysis of 3D coronary magnetic resonance angiograms. Magn Reson Med 2002;48(4):658–666.
25. Tello R, Crewson PE. Hypothesis testing. II. Means. Radiology 2003;227(1):1–4.
26. Medina LS, Zurakowski D. Measurement variability and confidence intervals in medicine: why should radiologists care? Radiology 2003;226(2):297–301.
27. Manke D, Nehrke K, Börnert P, Rösch P, Dössel O. Respiratory motion in coronary magnetic resonance angiography: a comparison of different motion models. J Magn Reson Imaging 2002;15(6):661–671.
28. Lustig M, Donoho D, Pauly JM. Sparse MRI: the application of compressed sensing for rapid MR imaging. Magn Reson Med 2007;58(6):1182–1195.
29. Börnert P, Koken P, Nehrke K, Eggers H, Ostendorf P. Water/fat-resolved whole-heart Dixon coronary MRA: an initial comparison. Magn Reson Med 2013 Feb 7. [Epub ahead of print]
30. Hu P, Chuang ML, Ngo LH, et al. Coronary MR imaging: effect of timing and dose of isosorbide dinitrate administration. Radiology 2010;254(2):401–409.
31. Danias PG, Roussakis A, Ioannidis JP. Diagnostic performance of coronary magnetic resonance angiography as compared against conventional x-ray angiography: a meta-analysis. J Am Coll Cardiol 2004;44(9):1867–1876.
32. Jahnke C, Paetsch I, Nehrke K, et al. Rapid and complete coronary arterial tree visualization with magnetic resonance imaging: feasibility and diagnostic performance. Eur Heart J 2005;26(21):2313–2319.
33. Yang Q, Li K, Liu X, et al. Contrast-enhanced whole-heart coronary magnetic resonance angiography at 3.0-T: a comparative study with x-ray angiography in a single center. J Am Coll Cardiol 2009;54(1):69–76.
34. Nagata M, Kato S, Kitagawa K, et al. Diagnostic accuracy of 1.5-T unenhanced whole-heart coronary MR angiography performed with 32-channel cardiac coils: initial single-center experience. Radiology 2011;259(2):384–392.
35. Knuesel PR, Nanz D, Wolfensberger U, et al. Multislice breath-hold spiral magnetic resonance coronary angiography in patients with coronary artery disease: effect of intravascular contrast medium. J Magn Reson Imaging 2002;16(6):660–667.